

## A NEW MODEL OF AC RESISTANCE IN ACSR CONDUCTORS

J.S. Barrett  
and  
O. Nigol, Senior Member, IEEE

Ontario Hydro, Research Division  
Toronto, Ontario

C.J. Fehervari, Student Member, IEEE  
and  
R. D. Findlay, Senior Member, IEEE

McMaster University  
Hamilton, Ontario

**Abstract** - An accurate new model for calculating AC resistance of ACSR conductors has been developed and verified for single, two and three layer conductor designs. Current redistribution was found to be far more important in determining the AC/DC resistance ratio than hysteresis losses in the steel core except in single layer conductors. The model suggests ways of reducing the AC resistance and promises to be a useful design tool.

### INTRODUCTION

In a recent IEEE task force report [1] it was shown that the measured AC resistance of ACSR conductors (aluminum conductor steel reinforced) sometimes exceeds values calculated by traditional methods. Three layer conductors were specifically identified as having AC/DC ratios up to 3 percent higher than the calculated values. Since the present worth of transmission line losses over a fifty year life is comparable to the capital costs of the line the extra AC resistance is very significant. Because of the uncertainty in the resistance value some power utilities tend to avoid using three layer ACSR conductors.

The usual method of calculating AC resistance of ACSR conductors is to apply skin effect and core loss corrections to the DC resistance value. The skin effect correction is determined by assuming the conductor to be a hollow aluminum tube [2-8]. The magnetic hysteresis and eddy current losses are usually determined by experimental means [5-12]. Some previous investigators [10,11,13] have indicated that the current density in ACSR conductors is not necessarily highest near the conductor's outer surface as the skin effect calculations predict. Previous models have evaluated core losses either as an equivalent resistance in a transformer circuit or as a correction to models that do not explicitly take these losses into account. The equivalent resistance method has the disadvantage that the core loss is associated with a particular layer of aluminum rather than the steel core and the correction method does not take into account the effect that core losses have on the current distribution in the aluminum. The model described in this paper takes core losses into account by means of a complex permeability for the steel core. As a result core losses are properly associated with the steel core and affect the current distribution in the aluminum.

85 SM 403-1 A paper recommended and approved by the IEEE Transmission and Distribution Committee of the IEEE Power Engineering Society for presentation at the IEEE/PES 1985 Summer Meeting, Vancouver, B.C., Canada, July 14 - 19, 1985. Manuscript submitted January 29, 1985; made available for printing June 7, 1985.

### The Model

The present model, like Morgan's [10], considers resistances, inductances due to longitudinal flux and inductances due to circular flux. These three elements are associated with the steel core and each aluminum layer as shown in Fig. 1. The total voltage drop as measured by a straight probe on the conductor surface is the same for every layer. Because of magnetic core losses, part of the voltage drop across the longitudinal inductance element in each layer is in phase with the layer current, thus making the element partially resistive. This inclusion of core losses as an inherent part of the model by means of a complex permeability rather than the real part alone and a different method of calculating inductances due to circular flux are what make the present model different from Morgan's. The treatment of the circular flux components is much simpler than some previous derivations [5,6].

The current in each layer of aluminum in Fig. 1 is calculated from the current density at the centre of the layer. The current in the steel core is calculated assuming a uniform current density equal to the surface density. The longitudinal inductance of the core is ignored because it is too small to significantly alter the current distribution in the aluminum. Details of the inductance calculations and constants in Fig. 1 are given in the appendix.

According to reference 5, 71% to 93% of the conductor current follows the helical paths of the wires and in most cases more than 85%. Some references [6,11,13,17,18] claim that the ratio is closer to 100%. The present model assumes that all of the current follows the helical paths in order to calculate the magnetic field in the steel core.

The complex permeability of the steel core was measured by two methods. The first was the usual method using a toroid made from the steel core. The second method was to calculate the magnetic field in the core using the measured current densities. The flux in the core was measured with a search coil as described below. Figure A2 in the appendix shows good agreement between the two methods at low values of magnetic field thus demonstrating that the helical path assumption is valid. One advantage of the present model is that it is dependent only on conductor geometry and the complex permeability of the steel core.

### Measurements

#### a) Search Coils

Fifty circular turns of insulated #22 wire were wrapped around the steel core and each layer of aluminum. These search coils provided direct measurement of the longitudinal components of flux. The steel core search coil measurements were used to obtain the complex permeability of the core which is examined in the appendix. The core characteristics obtained in this manner include both the hysteresis and eddy current loss contribution to core losses.

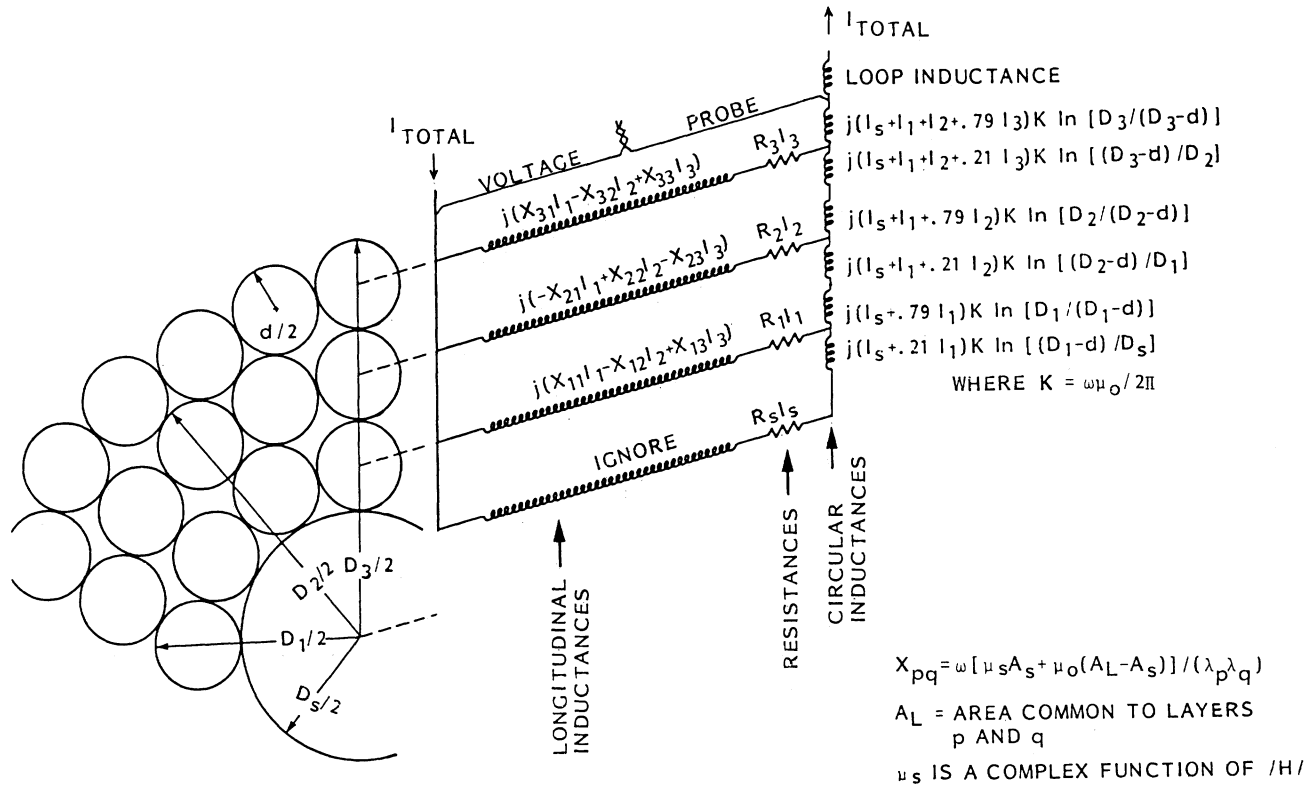


Fig. 1 Model of resistances and inductances for a 3-layer ACSR conductor.

b) Straight Voltage Probes

Straight voltage probes were installed on the outer surface of the steel core and each layer of aluminum. Contact was made by drilling small holes approximately half-way to the centre of the conductor wire and securing the ends of the probe wire in the holes with a small aluminum wedge. The #22 insulated wire traversed 5 lay lengths of each layer with both ends terminating on the same conductor wire.

The straight probe on the outer layer in Fig. 1 was used to determine the total AC resistance of the conductor. Using the total current measured by means of the current transformer (CT) as reference, the real part of the voltage drop measured by the straight probe is the resistive drop for the whole conductor. In theory this probe does not have to lie on the conductor surface because any extra loop area enclosed by the probe would result in an induced voltage which is 90 degrees out of phase with the total current. However, in practice, the extra flux could be affected by ferrous and conductive objects near the conductor, causing changes in the measured value of conductor resistance [15].

The straight probe measurements on other layers are not particularly useful except to serve as additional checks of the model.

c) Helical Current Density Probes

Probes following the helical path of the conductor wires and attached at the same points as the straight probes measure the following voltage [11-13,16]:

$$V = \int_{LOOP} \rho \vec{J} \cdot d\vec{l} + \frac{d\psi}{dt} \quad (1)$$

where  $\rho$  is resistivity,  $\vec{J}$  is current density and  $\psi$  is

magnetic flux. This equation is valid for any path chosen as illustrated in Fig. 2.

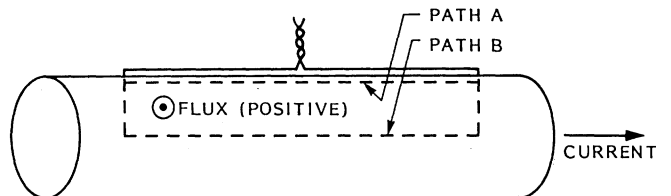


Fig. 2 Illustration of a current density probe following the path of a single conductor wire.

The probe in Fig. 2 gives a direct measurement of the current density in the part of the wire immediately adjacent to the path of the probe (path A). The reason is that the probe and path A form a loop that is too small to allow a significant amount of magnetic flux through it and so only the first term of equation 1 contributes to the measured voltage. It should be noted that the loop size and measured voltage are not functions of the depth of the probe contact points.

If path B is chosen, along the centre of the wire for example, equation 1 permits the current density at the centre of the wire to be calculated when the circular flux through the loop is known. Positive circular flux is shown in Fig. 2 for the current direction illustrated. The longitudinal flux is small enough to be ignored in this case.

Experimental Procedure

In preliminary tests a conductor loop 0.9 m wide and 3.9 m long was tensioned in a large steel frame.

Measurements of the longitudinal magnetic flux in the conductor were made with a movable search coil. These measurements indicated a peak value of flux at the centre of the test conductor with no truly constant region, gradually dropping to 96 percent of the peak value near the ends. Both circulating currents and magnetic flux were measured in the steel frame which was only 0.35 m from the conductor. Although the resistance values appeared to be reasonable there was some doubt about the influence of the steel frame on measured quantities. Measurement of large differences in current density of the different aluminum layers indicated that a thorough investigation was warranted.

A new experimental arrangement was erected in a 25 m test span as shown in Fig. 3. Only half of this length was used so that high current values could be obtained with the available power supply. The test conductor was a three layer 1192.5 kcmil (54/19) "Grackle" ACSR. Compression terminals were installed and the conductor tension was adjusted to 30 kN. The return conductor was of stranded copper and was laid on the floor which contained a large steel I-beam used as the magnetic return path. Losses in the I-beam are not a concern because external losses are not measured when the straight probe leads are attached to the surface of the conductor [15].

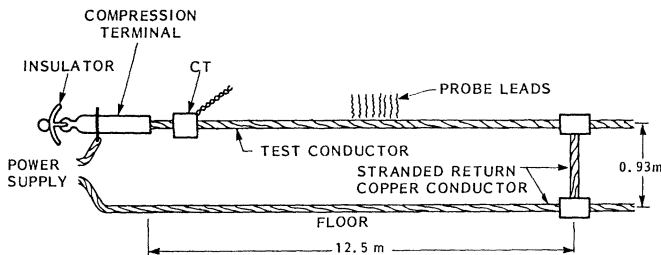


Fig. 3 Experimental Arrangement

Resistance measurements were made over a wide range of currents with a single straight voltage probe traversing 5 lay lengths of the outer aluminum layer. The probe was mounted in the centre region of the energized part of the conductor length with finely twisted leads to the oscilloscope which was approximately 3 m away to avoid the influence of magnetic fields on the scope. The probe length was measured within  $\pm 1$  mm (0.05%).

The uniformity of the longitudinal magnetic flux was measured with a movable search coil around the conductor. Less than 1% nonuniformity was measured along the test conductor except within 0.3 m from the ends of the energized section. Search coil measurements in the air confirmed that flux leakage was confined to the region approximately 0.3 m from the ends. A simple calculation shows that an air space of that width has a reluctance per unit length comparable to that of the small steel core (11.3 mm diameter) having a relative permeability of several hundred.

Large steel pedestals were inserted at the ends of the test section to complete the magnetic loop but they had no detectable effect on either the measured resistance or the longitudinal flux except very near the ends. These measurements demonstrate that the test setup was essentially a closed magnetic loop. This would also apply to a long 3-phase transmission line forming a closed 3-phase magnetic circuit with flux leakage occurring only at the ends. Detailed analysis shows that the leakage flux is of no concern and the B-H characteristics of the steel cores in both the test setup and in transmission lines are similar to those that would be measured for a complete loop of steel core.

The total conductor current was measured by means of CTs calibrated with magnitude accuracy of  $\pm 0.01\%$  and phase accuracy of  $\pm 5$  min over the range of cur-

rents used in the experiment. The current leads from the CTs to the scope were also twisted.

A digital storage scope was calibrated within  $\pm 0.1\%$  for both of its channels and was used to record simultaneous current and voltage waveforms on magnetic disks. Without the calibration, AC resistance errors were up to 2% because of differences in gain of the two channels. Phase angle error was 0.4 degrees which would have resulted in up to 0.5% error in AC resistance values. It was found that the scope errors could also be eliminated by interchanging the channels that recorded the CT and straight probe waveforms and repeating measurements at each conductor current value. By taking the square root of the product of the two  $\text{Re}(V)/I$  ratios the scope errors cancel. The waveforms were recorded 20 cycles after current of a preset level was established in order to avoid transient effects. In total, the 60 Hz current remained on for only 30 cycles to avoid heating the conductor.

Thermocouples were inserted under the outer and middle aluminum layers. Conductor temperatures never exceeded  $25^\circ\text{C}$  with an ambient room temperature of 21 to  $22^\circ\text{C}$ . Because of this small temperature rise, the corrections of measured resistances to  $20^\circ\text{C}$  were less than 2%.

After making resistance measurements for a full range of currents on the undisturbed "Grackle" conductor a compression terminal was cut off at one end of the sample and all of the aluminum wires were unwrapped to install probes on the steel core and aluminum layers. On each of them a search coil, straight voltage probe, helical current density probe and thermocouple were installed using tape to secure them in place. The main difficulty in restranding the conductor was in avoiding movement of the twisted probe leads from the underlying layers. After reassembly the conductor diameter in some places was larger than normal by nearly 1 mm. This was mainly due to the 50 turn search coils. One concern was that the probes would disturb the current distribution in the conductor. This was the main reason for first making measurements on the undisturbed conductor. A new compression terminal was installed after all the strands were in place and simultaneous current and voltage waveform were obtained and stored on magnetic discs over a wide range of currents. The current waveforms from the CT were paired with each probe waveform, using the total current as the reference.

After completing the measurements on the reassembled three layer "Grackle" conductor the whole procedure was repeated for two and single layer conductors obtained by removing successive layers from the "Grackle" conductor. Another sample of the "Grackle" conductor was used to obtain undisturbed two and single layer conductors. Although the resultant two and single layer conductors do not correspond to actual conductor designs their high steel-to-aluminum ratios make them well suited to the verification of the model.

#### Experimental Results

The resistances of the reassembled "Grackle" conductor with all probes installed agreed with those measured on the undisturbed sample within 0.5%. This is a good indication that the probes did not significantly alter the current distribution in the conductor.

Figure 4 is the vector diagram of the currents that the model predicts in each layer of the three layer "Grackle" conductor for a total current of 1608 A.

The correspondence between calculated and measured values is excellent. The largest discrepancy in magnitude is for the steel core, probably because the helical winding of the core results in a surface

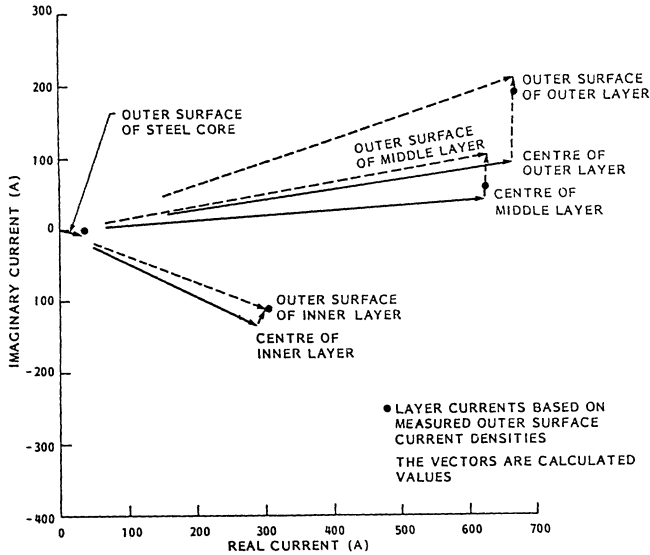


Fig. 4 Vector diagram of layer currents in "Grackle" ACSR at 1608 A total current. The currents predicted by the model are indicated by the vectors drawn in solid lines and are based on the calculated current densities at the centres of each aluminum layer and the surface of the steel core. The vectors drawn in dashed lines represent the currents based on calculated current densities on the outer surface of each aluminum layer. The points are the values based on the measured outer surface current densities.

density higher than the average density. As indicated in Fig. 1, this effect was ignored.

The other significant discrepancy is in the phase of the current in the middle layer. The most probable explanation of the discrepancy is the discovery, upon removing the outer layer of aluminum, that the helical probe on the middle layer had shifted over part of its length from the outer surface of the wire partially into the crack on one side of the wire. This explanation accounts for the placement of the measured middle layer point in Fig. 4 between the centre-of-layer and outer-surface vectors. The above effect was observed in the middle layer at all currents which would probably not be the case if the discrepancy were due to an error in steel core permeability. In retrospect it appears that the crack between the wires is a good place to position a current density probe to obtain a direct measurement of the average current density of a layer.

Figure 5 indicates the calculated and measured current densities at various points in "Grackle" conductor at 1608 A total current. The effect of the circular inductance is evident as a slight increase in current density on the outer surface of each layer and as a progressive increase of phase angle with distance from the centre of the conductor.

For the AC resistance of the conductor the most significant aspect is the redistribution of current, not to the outer layer of the conductor as traditional skin effect calculations would predict, but to the middle layer where the current density is 30% higher than in the outer layer and 24% higher than in the inner layer. In the two layer conductor formed by removing the outer layer of "Grackle" conductor the current density was only 2% higher in the outer layer than in the inner layer. Figure 14 of Reference 11 shows that the current density may be higher in the inner layer of a standard two-layer conductor. The major redistributions of current in the three layer conductor are due to the longitudinal inductances in

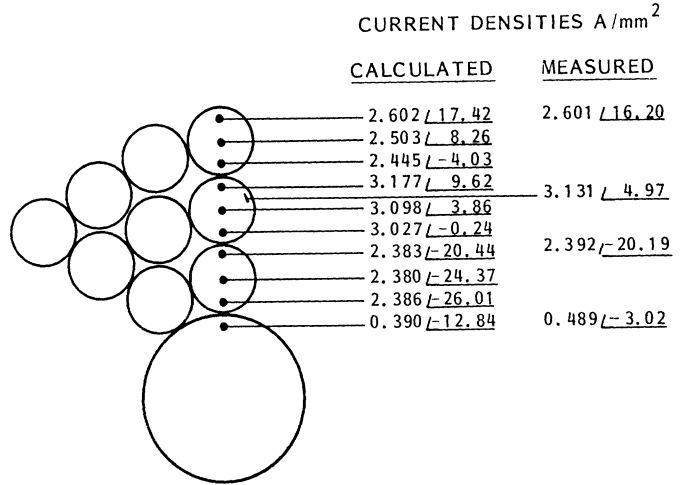


Fig. 5 Calculated and measured current densities in "Grackle" conductor at 1608 A total current.

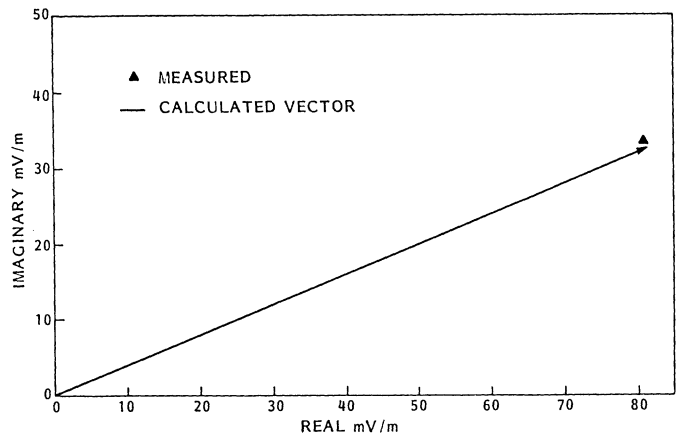


Fig. 6 Calculated and measured voltage per metre for the straight probe on the outer surface of "Grackle" conductor at 1608 A total current.

Fig. 1. This transformer effect is important because of the high magnetic permeability of the steel core.

Figure 6 shows the calculated vector and measured point for the straight probe voltage per metre on the surface of the conductor at 1608 A total current. The real part of this voltage divided by total current equals the conductor resistance. The calculated and measured values agree within 0.4%.

The total conductor resistance can be considered to be made up of three parts: the DC value, the increment due to current redistribution and the increment due to magnetic hysteresis and eddy current losses in the core. The measured and calculated total AC resistances are the real component of the straight probe voltage on the conductor's outer surface divided by total current. A DC resistance of  $46.80 \pm 0.05 \mu\Omega/m$  at 20°C was measured with a calibrated digital micro-ohm meter. It is important to note that some tables of calculated DC and AC resistances are based on the aluminum portion of the conductor alone, resulting in resistance values typically 2% higher than those with the core included. The Aluminum Association tables [8] are a good source of DC resistance values with the steel core included. The DC plus redistribution increment is calculated from the sum of  $I^2R$  losses in the steel core and each aluminum layer, divided by the square of total current. The magnetic core loss increment is the remaining portion.

Figures 7, 8 and 9 show the calculated and measured AC/DC resistance ratios as a function of current for the three layer "Grackle" conductor and the two and single-layer conductors derived from it by removing successive layers. The portions attributed to current redistribution and to magnetic core losses are also indicated. For "Grackle" conductor in Fig. 7 at 1608 A, current redistribution accounts for 6.0% of the increase over the DC value and magnetic core losses for 1.8% increase for a total AC/DC resistance ratio of 1.078 at 1608 A.

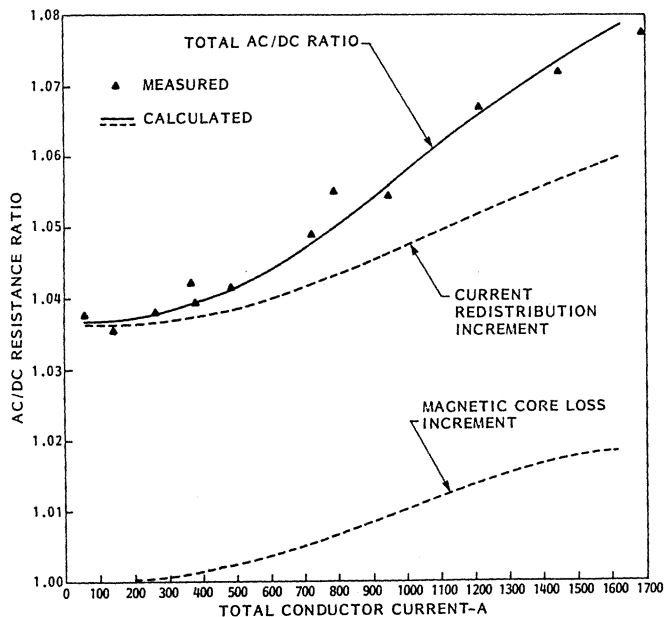


Fig. 7 Measured and calculated AC/DC resistance ratios for undisturbed three layer "Grackle" ACSR Conductor.

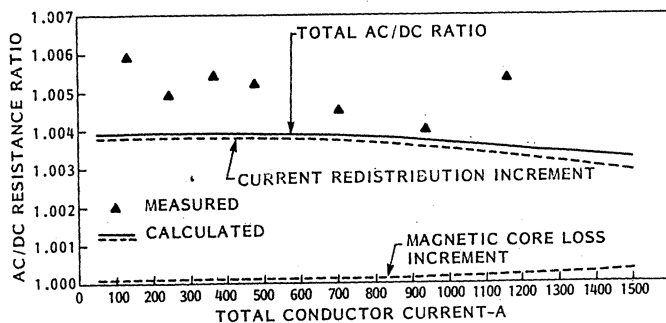


Fig. 8 Measured and calculated AC/DC resistance ratios for the undisturbed two layer ACSR conductor formed by removing a layer from "Grackle" conductor.

Figure 8 shows that the two-layer conductor made by removing the outer layer of "Grackle" conductor has an AC resistance only half a percent higher than the DC value in spite of its high steel-to-aluminum ratio of 0.23. These properties make such a conductor attractive for low sag and long span applications. The systematic difference between measured and calculated values is 0.1%. Better agreement should not be expected considering that the uncertainty in calibration of the oscilloscope-current transformer combination was 0.1%, in measured DC resistance also 0.1% and in probe length approximately 0.05%.

Figure 9 shows the AC/DC ratio of the single layer conductor formed by removing the outer two layers of "Grackle" conductor. As shown in the

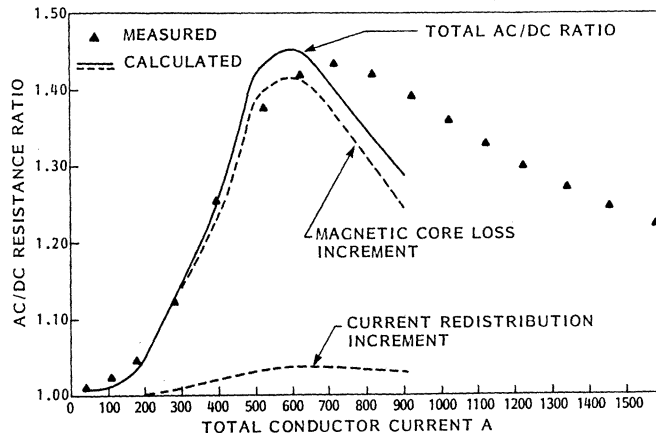


Fig. 9 Measured and calculated AC/DC resistance ratios for the undisturbed single layer ACSR conductor formed by removing the outer two layers from "Grackle" conductor.

appendix the magnetic properties of the steel core are significantly altered by its tensile stress when magnetic fields are higher than 1000 A/m. For the single layer conductor this occurs at approximately 350 A total current. It was not necessary to consider this effect in the three layer "Grackle" conductor in which the magnetic field is only 930 A/m at 1600 A total current or in the two layer conductor in which the field is 480 A/m at 1500 A total current. The discrepancy between measured and calculated values in Fig. 9 at high currents is due to ignoring the effects of the helical windings and circular flux within the steel core. However, the agreement is good in the normal range of operating currents.

#### CONCLUSIONS

An accurate model for calculating AC resistances of ACSR conductors has been developed. It supports the recent findings of the IEEE "Task Force on AC Resistance of ACSR" [1] with regard to one and three layer conductors. Current redistribution and magnetic core losses appear to be the dominant effects determining the AC resistance. Three and five layer ACSR conductors would become more attractive if the axial flux in the steel core could be reduced. This could be achieved either by appropriate adjustment of lay lengths [12] or by varying wire diameters in different layers. The model promises to be a useful design tool.

#### ACKNOWLEDGEMENTS

The authors gratefully acknowledge the contributions of Drs. M.A. Green and W.A. Chisholm for helpful discussions on electromagnetic theory and for their computer programming assistance. We also wish to thank G. Gouliaras for measuring the complex magnetic permeability of the steel core.

#### REFERENCES

- [1] D.A. Douglass and L.S. Rathbun, "AC Resistance of ACSR - Magnetic and Temperature Effects," Task Force of the IEEE Working Group on Calculation of Bare Overhead Conductor Temperatures, (B.S. Howington, Chairman), Paper 84-SM-700-1, IEEE Summer Power Meeting 1984.
- [2] H.B. Dwight, "Skin Effect and Proximity Effect in Tubular Conductors," AIEE Trans., Vol. 41, 1922, pp. 189-198.

- [3] H.B. Dwight, "Skin Effect in Tubular and Flat Conductors," AIEE Trans., Vol. 37, Part II, 1918, pp. 1370-1403.
- [4] A.E. Kennelly, F.A. Laws and P.H. Pierce, "Experimental Researches of Skin Effect in Conductors," AIEE Trans., Vol. 34, Part II 1915, pp. 1953-2021.
- [5] W.A. Lewis, P.D. Tuttle, "The Resistance and Reactance of Aluminum Conductors, Steel Reinforced," AIEE Trans., II, Vol. 77, 1958, pp. 1189-1210.
- [6] V.T. Morgan, "Electrical Characteristics of Steel-Cored Aluminum Conductors," Proc IEE, Vol. 112, No. 2, February, 1965.
- [7] V.T. Morgan, "The Current Carrying Capacities of Overhead Line Conductors," IEEE paper A78 575-3, Summer Power Meeting, 1978.
- [8] Aluminum Electrical Conductor Handbook, the Aluminum Association, Second Edition, 1982.
- [9] L.W. Matsch and W.A. Lewis, "Magnetic Properties of ACSR Core Wire," AIEE Trans., II, February 1969, pp. 1178-1189.
- [10] V.T. Morgan C.F. Price, "Magnetic Properties in Axial 50 Hz Fields of Steel Core Wire for Overhead-Line Conductors," Proc IEE, Vol. 116, No. 10, October 1969, pp. 1681-1694.
- [11] R.D. Findlay, "Analysis of Two Layer Aluminum Conductor Steel Reinforced," Paper C73 172-4, IEEE Winter Power Meeting 1973.
- [12] R.D. Findlay, "Equivalent Nonlinear Lumped - Parameter Network Representation for ACSR Conductors," IEE Proc, Vol. 127, Part C, No. 6, November 1980, pp. 430-433.
- [13] R.D. Findlay, and H. Riaz, "An Analysis of the Jarvis Crossing AACSR Conductor," Paper C72 191-0, IEEE Winter Power Meeting 1972.
- [14] R.D. Findlay and H. Riaz, "A Nonlinear Diffusion Model for the Electromagnetic Field Configuration of Single Layer ACSR," Paper A78 152-1, IEEE Winter Power Meeting 1978.
- [15] E.H. Salter, "Problems in the Measurement of AC Resistance and Reactance of Large Conductors," AIEE Trans., Vol. 67, 1948, pp. 1390-1397.
- [16] P.E. Burke and R.T.H. Alden, "Current Density Probes," IEEE Trans., PAS-88, No. 2, February 1969, pp. 181-185.
- [17] R. Goldschmidt, "The Resistance of Aluminum-Steel Cables to Alternating Current," CIGRE Paper 214, 1952.
- [18] K.R. Malayan, "Calculation of the Effective Resistance of Steel-Aluminum Conductors at Power Frequency," Izv., Akad., nauk Armyansk, SSR, Ser. tekhn. nauk, Vol. 24, pp. 58-66, 1971, (referred to by reference 7).

## APPENDIX

### 1. Inductances Due to Longitudinal Flux

Layers p and q have a common transformer core composed of the steel core and the air and aluminum

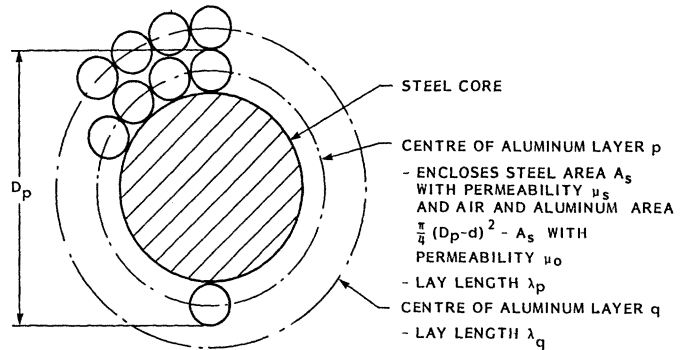


Fig. A1 Diagram for calculating mutual and self inductances due to longitudinal flux.

encircled by layer p. The magnetic flux that layer q produces within layer p is given by

$$\psi_{pq} = [\mu_s A_s + \mu_0 (\frac{\pi}{4}(D_p-d)^2 - A_s)] I_q / \lambda_q \text{ mWb} \quad (A1)$$

The voltage that this induces in layer p is given by

$$V_{pq} = j\omega \psi_{pq} / \lambda_p = j X_{pq} I_q \text{ V/m} \quad (A2)$$

The magnetic flux that layer p produces within layer q is given by

$$\psi_{qp} = [\mu_s A_s + \mu_0 (\frac{\pi}{4}(D_p-d)^2 - A_s)] I_p / \lambda_p \text{ mWb} \quad (A3)$$

The voltage that this induces in layer q is given by

$$V_{qp} = j\omega \psi_{qp} / \lambda_q = j X_{qp} I_p \text{ V/m} \quad (A4)$$

In equations A2 and A4, the mutual inductive impedances are given by

$$X_{pq} = X_{qp} = \omega [\mu_s A_s + \mu_0 (\frac{\pi}{4}(D_p-d)^2 - A_s)] / (\lambda_p \lambda_q) \quad (A5)$$

which defines the values in Fig. 1 and is also valid for the self inductance terms  $X_{pp}$  for which the product  $\lambda_p \lambda_q$  in the denominator is replaced by  $\lambda_p^2$ . The sign of the self inductances is always positive and the sign of the mutual inductances is positive if the layers are wound in the same direction and negative if they are wound in opposite directions.

It is important to note that  $V$ ,  $I_p$ ,  $I_q$  and  $\mu_s$  are complex quantities and  $\mu_s$  is a function of the magnitude of magnetic field  $H$  which, for a 3 layer conductor, is given by

$$H = 1000 (I_1 / \lambda_1 - I_2 / \lambda_2 + I_3 / \lambda_3) \text{ A/m} \quad (A6)$$

This equation assumes that the layer currents follow the helical wire paths. It is not apparent how to measure the direction of the current directly or to calculate the current leakage between layers or between wires in the same layer. The most convincing validation of the above assumption is the success of the model in describing current densities and the conductor resistance. The following section provides additional evidence.

2. The Magnetic Properties of the Steel Core

Figure A2 shows the real and imaginary components of the permeability of the steel core. A toroid of 1968 mm mean circumference was formed by butting the ends together and crimping a short steel compression fitting to join them. A 50-turn secondary of #22 copper wire was closely wound opposite the joint and a primary of 511 turns of #12 wire was wound over the whole toroid.

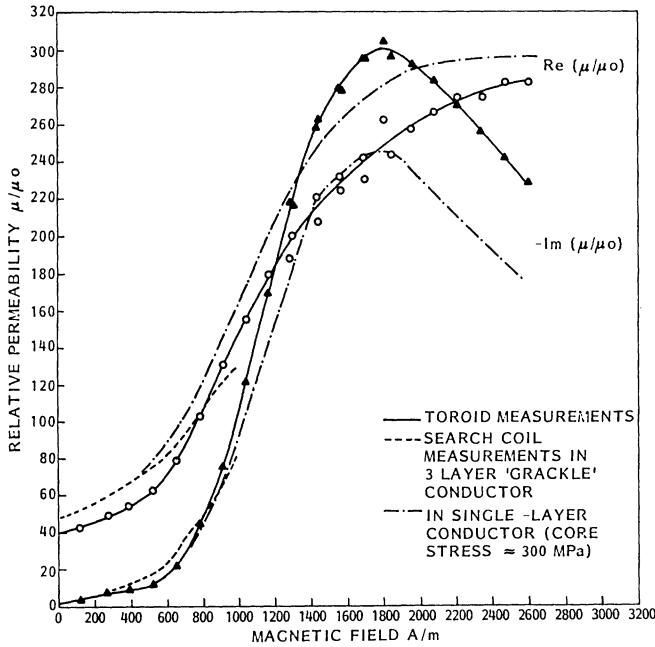


Fig. A2 Values of steel core permeability in the present experiment.

Figure A2 also shows the permeability obtained from the search coil measurements on the single and three layer ACSR conductors. The voltage of the 50 turn search coil on the steel core is given by

$$V = 50j\omega A_s \mu_s H / 1000 \text{ mV} \tag{A7}$$

With the aid of equations A6 and A7 the complex values of H and  $\mu_s$  can be determined as a function of the magnitude of H from the measured values of V. The layer currents used in equation A6 were taken from the measured outer surface current densities with a circular flux correction to obtain the current densities at the centres of the layers. The agreement between the toroid measurements at low magnetic field values is further confirmation of the helical path assumption.

The magnitude of  $\mu_s$  varies throughout each cycle but the calculation method described here is based upon rms values of current and results in permeability for an rms value of H. The magnetic core losses are composed of hysteresis losses due to magnetic domain reorientation and eddy current losses induced mainly by longitudinal flux in the core. Both losses are included in the imaginary component of permeability measured at 60 Hz. Use of a complex permeability makes the approximation that the B-H curve is elliptical in shape. This approximation is acceptable for loss calculations as demonstrated by Figs. 7-9.

For the two and three layer conductors the magnetic field was less than 1000 A/m over the full cur-

rent range and the following equations describe the magnetic permeability in this range.

$$\text{Re}(\mu_s) = (40 - 0.0243|H| + 0.000137|H|^2)\mu_0 \tag{A8}$$

$$\text{Im}(\mu_s) = -(5 + 1.03 \times 10^{-10}|H|^4)\mu_0 \tag{A9}$$

The calculations for Fig. 9 were based on the permeability measured on the reassembled single layer conductor sample with current density probes, voltage probes and search coils installed. The curves in Fig. A2 for 1 and 3 layer conductors were obtained at 30 kN tension. For the single layer conductor this corresponds to approximately 300 MPa tensile stress on the steel core alone. The effect of this tension is very similar in magnitude to that reported in Fig. 7 of reference 10 for 33 kg/mm<sup>2</sup> (323 MPa) tensile stress.

3. Inductances Due to Circular Flux

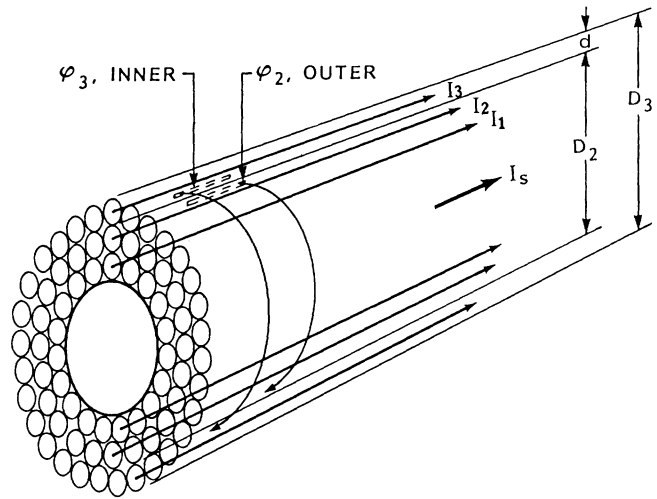


Fig. A3 Diagram for calculation of inductances due to circular flux.

As a first approximation the layer currents are assumed to be concentrated at the centre of each layer as illustrated in Fig. A3. In other words, each layer is treated as a thin uniform cylinder. In this approximation each layer produces flux only outside itself.

The fluxes illustrated in the figure are given by

$$\psi_{2, \text{OUTER}} \approx \frac{(I_s + I_1 + I_2)}{2\pi} \mu_0 \ln [D_2 / (D_2 - d)] \tag{A10}$$

and

$$\psi_{3, \text{INNER}} \approx \frac{(I_s + I_1 + I_2)}{2\pi} \mu_0 \ln [(D_3 - d) / D_2] \tag{A11}$$

Since the currents are not actually concentrated at the centre of each layer the contribution of  $I_2$  to  $\psi_{2, \text{OUTER}}$  has been overestimated and  $I_3$  makes a contribution to  $\psi_{3, \text{INNER}}$  which has not been taken into account. These discrepancies can be corrected as follows.

Figure A4 illustrates the method of calculating the circular flux that a layer produces within its own inner and outer portions. By assuming a uniform current distribution over each wire's cross section, and integrating the flux, it is found that the current makes a 21% contribution to the inner flux and a 79% contribution to the outer flux. These corrections are included in the model as described by Fig. 1. A minor correction to phase has been ignored.

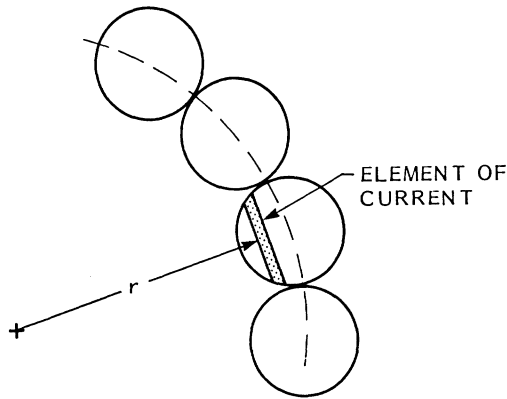


Fig. A4 Illustration of correction to circular flux calculation.

#### 4. Solution of the Equations

The model equations were solved using the "TK Solver" program on an IBM PC. Each equation was carefully divided into real and imaginary components and the "TK Solver" iterated on all of the unknown variables until consistency was achieved. The initial conditions for iteration were based on uniform DC current densities and voltage drops. There are three basic requirements for solving the model equations. The first is that the four currents  $I_s$ ,  $I_1$ ,  $I_2$  and  $I_3$  must add up to the total current. The second is that according to Kirchoff's law the total voltage drop shown for the straight probe in Fig. 1 must be the same for all four current paths. The third constraint is that the longitudinal inductances used in Fig. 1 must be consistent with their definition in terms of the layer currents as given by equations A5, A6, A8 and A9. Another version of the program is being written in APL.

#### 5. Nomenclature and Units

S.I. units are used throughout with prefixes chosen for convenience in recording measured values and to avoid powers of ten in equations whenever possible. Unless otherwise stated in the text the units are as follows

$\rho_s, \rho_a$  steel and aluminum resistivities,  $\Omega \text{mm}^2/\text{m}$   
 A cross sectional areas  $\text{mm}^2$   
 D outer diameters of layers, mm

d aluminum wire diameter, mm  
 $\lambda$  lay lengths, mm  
 R layer resistances,  $\Omega/\text{m}$   
 J current densities,  $\text{A}/\text{mm}^2$   
 $\psi$  magnetic fluxes, mWb (mWb/m for circular)  
 V voltage drops per unit length, V/m  
 H magnetic field, A/m  
 $\mu$  magnetic permeability, H/m  
 I currents, A

#### 6. Conductor Parameters Used in the Model

##### Resistivities

$\rho_s = 0.1775 + 0.0002 \Omega \text{mm}^2/\text{m}$   
 $\rho_a = 0.02818 + 0.00002$  (measured values corrected to  $20^\circ\text{C}$ )

##### Areas

$A_s = 76.58 \text{ mm}^2$   
 $A_1 = 134.28 \text{ mm}^2$   
 $A_2 = 201.42 \text{ mm}^2$   
 $A_3 = 268.56 \text{ mm}^2$

##### Outer Layer Diameters

$D_s = 11.3 \text{ mm}$   
 $D_1 = 18.9 \text{ mm}$   
 $D_2 = 26.4 \text{ mm}$   
 $D_3 = 33.9 \text{ mm}$

##### Aluminum Wire Diameter

$d = 3.77 \text{ mm}$

##### Lay Lengths

$\lambda_s = 187.4 \text{ mm}$   
 $\lambda_1 = 291.6 \text{ mm}$   
 $\lambda_2 = 365.0 \text{ mm}$   
 $\lambda_3 = 400.0 \text{ mm}$

$\mu_o = 4\pi \times 10^{-7} \text{ H/m}$

##### DC Resistances of Layers

$$R = (\rho/A) \sqrt{1 + \left[ \frac{\pi(D-d)}{\lambda} \right]^2} \quad \Omega/\text{m}$$

(The -d term is omitted for steel)

##### Temperature Coefficient of Resistivity

$\alpha = 0.00404 \text{ }^\circ\text{C}^{-1}$  for small corrections of measured resistance (<2%)

### Discussion

**Vincent T. Morgan** (CSIRO Division of Applied Physics, Sydney, Australia): The increasing cost of energy losses has fostered a renewed interest in the losses of steel-cored conductors, and the authors have contributed a welcome addition to the literature on the subject. The use of a helical probe is an interesting technique to measure the current distribution within a single wire: have the authors made any measurements of the current distribution between the wires in the same layer?

We have found that the straight surface probe is susceptible to induced voltages from external fields, and that greatly reduced induction occurs when two similar parallel horizontal conductors are tensioned and shorted at one end to form a current loop. The potential taps are made in pairs at each end of the lengths of the conductor, and the measuring leads are twisted; they run in the plane of the conductors and equidistant from them up to the center of the lengths. The leads are then taken away at right angles to the plane of the conductors. The sum of the voltage drops across the two lengths of the conductor is found from the difference between the potentials measured at each pair of taps, i.e., those around the long loop and the short loop.

The use of longitudinal and helical probes and the dismantling and reassembly of the conductor would be expected to disturb the electrical contacts between adjacent layers, but the authors' results do not show any marked discrepancy. This may be because the sample length was short, so that current distribution between layers occurred at the end compression clamps. The layer currents were measured at near-ambient temperature: if this current distribution were also to occur at operating temperatures, say up to 80°C, one would expect some distortion of the radial temperature distribution. Since this is not seen in practice, it suggests that the current distribution between layers may vary with temperature and tension.

The measured ac-dc resistance ratio versus current characteristic for the three-layer conductor lies above most of the experimental data given in Ref. [1]. Would the authors please comment on this.

The analytical method used to calculate the redistribution of current between the layers is similar to that of [10], apart from the refinement in the calculation of the circular fluxes. The calculated layer currents are qualitatively similar to those in [10]. It should be noted that the modulus of the complex permeability, not the real part, was used in [10]. The search coil method of measuring the permeability of steel wires measures the surface value. The actual permeability is reduced by the shielding effect of eddy currents. This reduction depends on the magnetic induction, the mechanical tension, and the temperature, and can approach 35 percent [10].

Manuscript received July 23, 1985.

**Dale A. Douglass** (Power Technologies, Inc., Schenectady, NY): The authors are to be congratulated on producing a carefully researched paper on a subject that is of interest to both conductor and transmission line designers — namely, the ac resistance of the ACSR conductor. I wish to pose a few questions and to present some comments on the use of the authors' work.

The ac resistance of *single*-layer ACSR conductors has been determined by extensive measurements, since the magnetic core losses are significant (in excess of 10% at moderate electrical loading) and are difficult to calculate.

The ac resistance of ACSR conductors having *two or four* aluminum strand layers, may be calculated with considerable accuracy by including temperature and skin-effect corrections, as described in the Task Force paper on ac resistance (Ref. [1]) or in the *Aluminum Electrical Conductor Handbook* (Ref. [2]).

The ac resistance of *three*-layer ACSR may be calculated in the same manner as for "even"-layer ACSR, if after doing so, the magnetic core losses are accounted for by a multiplier. This magnetic loss multiplier was considered in some detail in Ref. 1. However, it should be noted that for three-layer ACSR, the magnetic core losses are much less important than for single-layer ACSR, the ac resistance being increased by only a few percent.

Ref. 1 analyzed a large number of experimental measurements of ac resistance for a variety of strandings to derive a linear regression curve of the ratio of *measured* ac resistance to *calculated* ac resistance, which included skin effect but not magnetic core losses. Using the results of this paper, one can calculate the ac resistance of three-layer ACSR quite easily.

For example, consider a Grackle conductor with 1260 amperes at a temperature of 75° C. From Table 4-16 in Ref. 2 (or by calculations based on ASTM Standard B232), the dc resistance at 20° C is 0.0760 ohms/mile.

This is corrected to 75° C by multiplying by  $(1.0 + 0.00404 \cdot (75 - 20)) = 1.222$ . The skin effect multiplier is found from Fig. 3-8 of Ref. 2. It is 1.019. For a current density of 1060 amperes per million cmils (1260 amps divided by 1192.5 kcmils), Ref. 1 indicates a multiplier of 1.040. The calculated ac resistance is therefore:

$$0.0760 \cdot 1.222 \cdot 1.019 \cdot 1.040 = 0.0984 \text{ ohms/mile.}$$

The calculated ac-dc resistance ratio of the Grackle conductor, based on Refs. 1 and 2, is therefore 1.061 ( $1.019 \cdot 1.040 = 1.061$ ).

According to Fig. 7 the authors calculated for the Grackle conductor an ac-dc ratio of 1.067 at a current of 1260 amperes. As the authors suggest, agreement between the standard calculation method (using the magnetic core loss multiplier of Ref. 1) and their work appears to be quite good.

To explore this further, consider Fig. 1 of this discussion. This rather busy figure compares the authors' ac-dc ratio for the Grackle conductor (given in their Fig. 7) to the ac-dc ratio calculated by the standard method. Note that the total ac-dc ratio curves are quite close—up to about 1200 amperes—but they appear to diverge for higher currents, where the "magnetic core loss" becomes more important.

Since the total ac-dc curve developed from the task force paper is based on a large number of measurements on an equally large number of conductors, the agreement with the authors' data serves to support their work. However, the agreement also suggests the use of the relatively simple standard calculation method presented in Refs. 1 and 2 rather than the more complex method presented by the authors. In particular, for the electrical loss calculations used for transmission line conductor selection, it is difficult to imagine the need for a more complex method of calculating ac resistance, considering the uncertainties in estimating conductor temperature over the life of the line. However, the more complex analytical method developed by the authors may be of use in conductor design if small adjustment of lay lengths can affect the ac resistance significantly. Would the authors comment on the use of their analytical model? Do they have any estimates of how sensitive the ac resistance is to lay length? Also, what were the lay lengths of the "Grackle" conductor tested?

Finally, in preparing Ref. 1, it was noted that the ac-dc resistance ratio decreased in an erratic fashion for current densities in excess of 1600 amperes/million cmils, so that a typical correction curve could not be derived beyond that current density. The ac-dc ratio plotted in Fig. 7 considers current densities up to 1425 amperes per million cmils (1700 amperes in the Grackle conductor). While this is certainly adequate for the normal operation of this conductor, did the authors look at higher current densities? Does their analytical model suggest the cause of the wide variation in ac-dc ratio at higher current densities with three-layer ACSR?

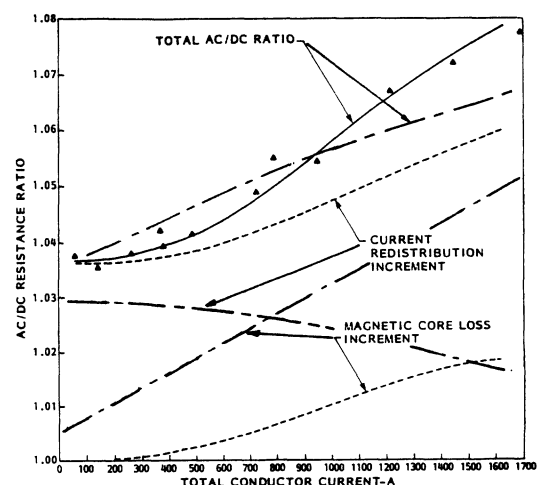


Fig. 1. Comparison of calculated ac-dc resistance ratios for "Grackle" 54/19 ACSR. Curves indicated by "—" are calculated by method of Refs. 1 and 2 of this discussion. Other curves are from Fig. 7 of the paper.

## REFERENCES

- [1] D. A. Douglass and L. S. Rathbun, "AC Resistance of ACSR Magnetic and Temperature Effects," Task Force of the IEEE Working Group on Calculation of Bare Overhead Conductor Temperatures, (B.S. Howington, Chairman), Paper 84-SM-700-1, IEEE Summer Power Meeting, 1984.
- [2] *Aluminum Electrical Conductor Handbook*, the Aluminum Association, Second Edition, 1982.

Manuscript received August 12, 1985.

**J. S. Barrett, O. Nigol, C. J. Fehervari, and R. D. Findlay:** We would like to thank Dr. Morgan for his comments and to express our compliments on his many useful and thought-provoking papers relating to ampacity and electrical properties of ACSR conductors.

We have not looked for differences between current densities in different wires of the same conductor layer because there is no reason to expect significant variations. Since any given wire has translational symmetry with respect to the other wires in the same layer, the only differences might be in contact resistance with adjacent wires. However, if contact resistances were low enough to play a significant role, the measured current densities and resistances would not agree so well with a model that assumes that all of the current follows the helical paths of the wires. Measured current densities of essentially randomly selected wires of all layers of one-two-, and three-layer conductors have been in excellent agreement with the model. This confirms that the variation of current in wires of the same layer is small.

We disagree with the statement that the straight surface probe is susceptible to induced voltages from external fields. Indeed, Salter [15] has demonstrated that an arrangement such as the one used by Dr. Morgan, with the probes not mounted on the conductor surface, is much more susceptible to external fields. Fig. 6 in our paper shows a voltage measured by a surface-mounted probe, which is in good agreement with the model calculation. The imaginary part of this voltage is the inductive drop due to the internal inductance of the conductor. The method proposed by Dr. Morgan would include the external loop inductance of the conductor, and so the imaginary part of the voltage and its associated error would be many times larger than what we measured. In addition, all flux passing through the conductor loop between the two probes contributes to the measured voltage. Because of the large size of this loop, such an experimental arrangement is very susceptible to external fields. It is better to exclude the external inductance of the conductor as we did, by using a probe mounted on the conductor surface.

We also disagree with Dr. Morgan's suggestion that the lack of discrepancy between reassembled and undisturbed conductors might be due to short sample length and that the current distribution might have been established by the end clamps. The end clamps contain a large amount of aluminum, and they compress the aluminum wires into a solid mass without air gaps. The current distribution in such a mass is expected to be highest on the outer surface of the clamp due to the skin effect. In contrast, the current density of the three-layer conductor was highest in the middle layer by approximately 27 percent. As discussed in the paper, measurements of the longitudinal magnetic flux had stabilized within approximately 30 cm of the ends of the sample, and all the current and voltage probes were approximately 5 m from the ends. The fact that the model worked for three different conductors is also a good indication that the sample was long enough for the current to redistribute from whatever its distribution in the clamps to the distributions measured at the centers of the samples.

While it may be true that the current distribution might change somewhat with temperature and tension, the radial temperature distribution is not a sensitive way to measure the effect because the temperature profile is not a sensitive indicator of where the heat is produced. For example, the three-layer Grackle conductor has approximately 27 percent more current per wire in the middle layer than in the other layers. This would produce approximately 60 percent more heat per wire in the middle layer than in the other layers. However, the temperature will still be highest in the steel core, and in general, a very careful measurement of the temperature derivatives would be necessary to determine the current distribution.

Fig. 5 of Ref. [1] indicates an average resistance multiplier of 1.04 at 1 A/kcmil. Since this factor is applied in addition to a skin effect of approximately 3 percent at room temperature, the total ac-dc resistance ratio at that current density is approximately 1.07. From our Fig. 7, the total ac-dc resistance ratio for the "Grackle" (1192.5 kcmil) conductor

at 1192.5 A is approximately 1.065, which is in fairly good agreement with Ref. [1]. However, it is important to note the scatter in the data of Ref. [1]. Although we do not know how much of the scatter is due to experimental error, our model calculations show that fairly small changes in the lay lengths produce large changes in the ac resistances. As a result, none of the data in Figs. 2-5 of Ref. [1] would be unreasonable.

We agree with Dr. Morgan that our model is similar to his [10], and indeed we pointed out the similarities and differences in the paper. His equations were presented as a means of calculating steel core losses along without mention of current redistribution losses. In contrast, our model, with its easily grasped pictorial representation, gives a comprehensive and accurate description of the electrical behavior of ACSR conductors. It is regrettable that Dr. Morgan did not develop his model further instead of reverting to the traditional method in his more recent publications. In his model there appear  $\sin\theta$  values for each layer (Eq. 27-33) that are numerically equal to  $\cos\delta$  where  $\delta$  are the loss angles given in his final example. As a result,  $\mu_0\mu_a\sin\theta$  is the real part of the magnetic permeability. However, in an accurate model it is important to retain both the real and imaginary parts of the permeability, fluxes, and inductances. It should also be noted that  $\mu$  and  $\delta$  of the steel core do not have separate values for each aluminum layer but are single functions of the total magnetic field of all the layers.

As we stated in the paper, the two methods we used to measure magnetic permeability include the effects of eddy currents. This is desirable because it allows hysteresis and eddy current losses to be calculated together with a single complex  $\mu$  value. The effect of tension was also noted in our data presented in the appendix.

The authors also wish to thank Mr. Douglass for his comments and questions and to note that the task-force paper by him and Mr. Rathbun on ac resistance of ACSR [1] has become a useful reference point for further study.

The ac resistance of *single-layer* conductors need not rest solely on experiment but can be calculated, as Fig. 9 demonstrates. Although there is room for refinement of the model in this case, the new method is reasonably accurate except at very high current densities where the ac-dc resistance ratio exceeds approximately 30 percent.

The ac resistance of *two- and four-layer* conductors are not necessarily calculated accurately by the traditional skin-effect graphs. The two-layer conductor discussed in our paper would have an ac-dc resistance ratio of 1.010 according to the traditional method, but the transformer effect of well-balanced lay lengths makes the current density highly uniform so that the actual ac-dc resistance ratio is only 1.005. According to our model calculations, the imbalance of lay lengths allowed by present standards could result in ac-dc resistance ratios of 1.03 or higher in two-layer conductors. Dr. Morgan cites several references confirming this result in his discussion of [1].

The graph that Mr. Douglass presents presents in his discussion shows that the average ac-dc resistance ratio of *three-layer* ACSR conductors, as calculated according to [1], are in agreement with our experimental values for a particular sample of "Grackle" conductor having the lay length values given in the appendix to our paper. However, the figure also makes it clear that our model differs radically with the method of [1] in its description of the two resistance increments that make up the total ac-dc ratio. Mr. Douglass appears to be asking whether or not, in view of the agreement between total ratios, we should continue to use the traditional skin-effect method and a magnetic core loss multiplier. Our answer is no.

First of all, the basic assumptions of the skin-effect method are incorrect. The three-layer ACSR conductor does not behave as a solid tube with the highest current density on the outer surface. As a result, the current redistribution losses calculated on the basis of that assumption are not in agreement with measured values. The magnetic core loss multiplier does not really represent core loss but actually represents the average discrepancy between an incorrect skin effect and measured total resistance.

A second reason why we should not continue to use the traditional method corrected with a multiplier is that lay lengths are important. Our model calculations show that variations of lay lengths within the values specified by present standards could account for the scatter in the data of Ref. [1]. Our calculations also indicate that the three-layer ACSR conductor, the size of the "Grackle," can be designed with an ac-dc resistance ratio less than 1.015 for currents as high as 1700 A. This is a 2-6 percent improvement over Fig. 7 and represents a large economic benefit. We intend to test new low-loss conductors soon.

At 1700 A, the Grackle conductor we tested was still far from magnetic saturation. We have not examined higher currents and have no explanation for the erratic behavior at high currents mentioned by Mr. Douglass.

It is our opinion that, in light of our results, the traditional skin-effect calculation as applied to ACSR conductors should be discontinued. The traditional skin-effect method is based upon the assumption that stranded ACSR behaves like a solid tube, resulting in a high current density on the conductor surface. However, in fact, the actual current distribution is strongly affected by the lay lengths of all the layers. The traditional skin-effect method is not even accurate for two-layer conductors. It is necessary to specify the lay lengths of each aluminum layer of ACSR conductors to calculate the ac resistances. It would be well worthwhile for utilities to consider this in light of the large economic benefit of a few percent reduction in losses and to incorporate specific lay lengths in the conductor standards.

Manuscript received September 5, 1985.